Atomic structure of solid and liquid polyethylene oxide

J. A. Johnson, M.-L. Saboungi,[a] D. L. Price, and S. Ansell
Argonne National Laboratory, Argonne, Illinois 60439

T. P. Russell
Polymer Science and Engineering Department, University of Massachusetts, Amherst, Massachusetts 01003

J. W. Halley and B. Nielsen
Department of Physics, University of Minnesota, Minneapolis, Minnesota 55455

(Received 23 April 1998; accepted 23 July 1998)

The structure of polyethylene oxide (PEO) was investigated by neutron scattering in both semicrystalline and liquid states. Deuterated samples were studied in addition to the protonated ones in order to avoid the large incoherent scattering of hydrogen and identify features in the pair correlation functions attributable to C–H pairs. Analysis of the deuterated sample gave additional information on the C–O and C–C pairs. The results are compared with molecular-dynamics simulations of liquid PEO. © *1998 American Institute of Physics.* [S0021-9606(98)51440-7]

I. INTRODUCTION

Polyethylene oxide (PEO) is a leading candidate for the electrolyte in lithium polymer batteries.[1–5] In practical applications, such systems are operated at temperatures above the glass–liquid transition but where sufficient interchain entanglement exists to form a rubbery material. In this state, the material contains both crystalline and amorphous regions: the Li conduction is believed to take place in the latter.[6,7] The crystal structure of PEO is well known from x-ray and neutron diffraction:[8,9] the unit cell consists of seven ($O–CH_2–CH_2$) repeat units which have an extended helical structure of length 19.3 Å over two turns of the helix. Small-angle neutron scattering has provided information about the chain conformation.[10] However, no experimental information about the structure of the amorphous phase at the atomic level is available. Recently, Lin *et al.*[11] carried out a molecular-dynamics (MD) simulation of amorphous PEO, the ultimate goal being to investigate lithium ion transport in this polymer. Because the polymer electrolytes of interest are between their glass and melting temperatures, the amorphous regions are not at equilibrium and one lacks the criterion of equilibrium in evaluating the validity of a molecular-dynamics model. To produce a model of these nonequilibrium amorphous regions which could be expected to reasonably simulate the amorphous regions of the real system, Lin *et al.* computationally polymerized a MD model[12] of monomeric dimethyl ether liquid. While not intended to be a fully realistic simulation of the amorphous chains in the interlamellar region, the simulations represent a plausible working model of the amorphous component of PEO. The nonequilibrium state of the amorphous chains, however, means that the observed states will be history dependent even if the atomic force model is a perfect representation of the real system; further validation of the model is required.

In this paper results are presented for the atomic structure of PEO in the semicrystalline (at room temperature) and liquid (at 90 °C) states as a first step toward structural measurements of lithium-salt-PEO solutions. The results were obtained using time-of-flight neutron scattering at a pulsed neutron source, which provides data over a wide range of scattering vectors from which pair distribution functions with good spatial distribution can be derived. A method for taking account of the presence of hydrogen in the MD model has been developed, while still using the united atom model for the dynamics in order to compare the neutron scattering results with the model. Within these constraints, the calculations are in excellent agreement with the measurements.

II. EXPERIMENTS

Deuterated (D-PEO) and protonated (H-PEO) samples were synthesized as described by Eisenbach *et al.*[13,14] with two different molecular weights (1.4×10^4 and 1.27×10^5). About 2 g of each sample were loaded into 6 mm diameter vanadium containers. Time-of-flight neutron diffraction measurements were performed at the GLAD facility at the Intense Pulsed Neutron Source. Runs were carried out for 24 h at room temperature on each sample, and for shorter times on the empty vanadium containers, the instrument background, and a vanadium standard rod for intensity calibration. Subsequently, the two D-PEO materials were combined and measured in the liquid state at 90 °C for 22 h.

The diffraction data were corrected for background and container scattering, multiple scattering, and absorption using standard methods. For the D-PEO samples the scattered intensity was combined over a wavelength λ range of 0.33–4.0 Å and a scattering angle 2θ range of 8°–125°; for the H-PEO the 2θ range was reduced to 8°–50° because of problems related to the large effect of inelastic scattering associated with hydrogen which cannot be estimated reliably by the usual Placzek procedure. The self-scattering was approximated by fitting Chebyshev polynomials to the total scattered

[a]Author to whom correspondence should be addressed. Electronic mail: mls@anl.gov

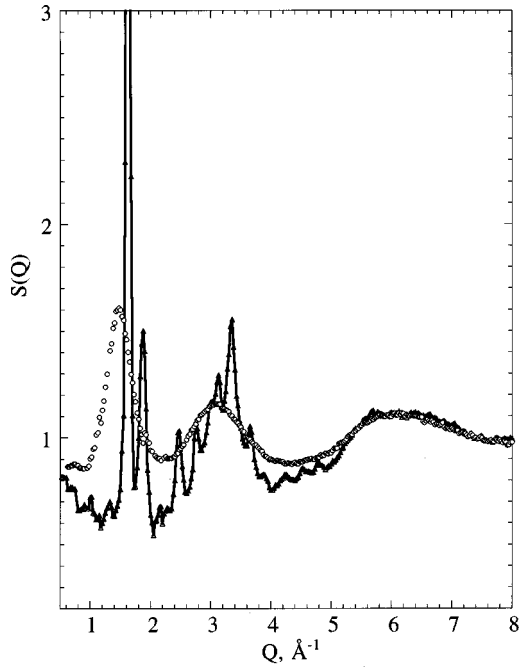

FIG. 1. Neutron-weighted average structure factors of D-PEO at RT (triangles) and at 90 °C (open circles).

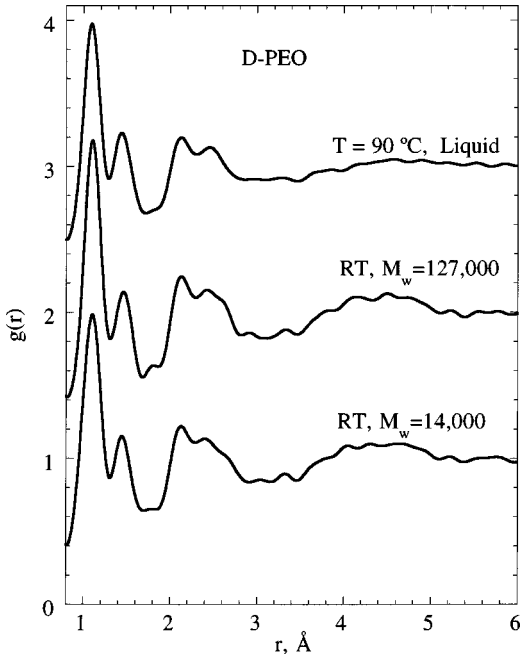

FIG. 2. Neutron-weighted average pair correlation functions for D-PEO. The upper curve has been moved up by two units and the middle curve by one unit for clarity.

intensity and then subtracted, yielding the interference scattering $I(Q)$ and the neutron-weighted average structure factor $S(Q)$:

$$I(Q)=\langle b\rangle^2[S(Q)-1]=\sum_{ij} c_i c_j b_i b_j[S_{ij}(Q)-1], \quad (1)$$

where $\langle b\rangle=\Sigma_i c_i b_i$, b_i and c_i are the coherent scattering length and concentration of species i, respectively, and $S_{ij}(Q)$ is the partial structure factor for the element pair (i,j). In addition, an H-D first-order difference calculation was performed, given by

$$I_{\mathrm{D}}(Q)-I_{\mathrm{H}}(Q)=2c_{\mathrm{H}}(b_{\mathrm{D}}-b_{\mathrm{H}})\sum_j c_j b_j[S_{\mathrm{H}j}(Q)-1], \quad (2)$$

where I_{D}, I_{H} are the corrected interference scattering measured for the D- and H-PEO and $S_{\mathrm{H}}(Q)$ is the hydrogen-difference structure factor describing the average environment of the hydrogen atoms.

III. RESULTS

The structure factors for D-PEO at room temperature and 90 °C are shown in Fig. 1; since there is very little difference between the results for the two samples with different molecular weights, data are shown only for one sample at room temperature. The partial crystallinity at room temperature is evident from the presence of Bragg peaks; on heating to 90 °C, these peaks disappear and the sample becomes completely amorphous. The structure factors were Fourier transformed with a maximum entropy procedure[15] to give the neutron-weighted average pair correlation function

$$g(r)=\frac{1}{2\pi^2\rho_0 r}\int_0^\infty [S(Q)-1]Q\,\sin\,QrM(Q)dQ+1, \quad (3)$$

where $M(Q)$ is the Lorch window function and ρ_0 is the total number density taken as 0.115 and 0.10 $\times 10^{24}$ atoms/cm^3 at room temperature and at 90 °C, respectively. The upper cutoff of $M(Q)$, Q_{cut} was taken as 30.0 and 16.1 Å^{-1} for the D and H samples, respectively. To derive coordination numbers, Gaussian functions convoluted with the transform of the Lorch window function were fitted to the measured total correlation function

$$T(r)=4\pi\rho_0 r g(r). \quad (4)$$

If a peak in $T(r)$ can be associated with a given pair (i,j), the area of the corresponding peak in $rT(r)$ is equal to the product of the coordination number $C_i(j)$ and the weighting factor $c_i b_i b_j/\langle b\rangle^2$.

The pair correlation functions for D-PEO at room temperature and 90 °C are shown in Fig. 2. By analogy with the crystal structure, the peak at 1.1 Å is attributed to the C–D atom pair, the peak at ~1.45 Å to a mixture of C–O and C–C correlations, and the small peak at 1.75 Å to D–D correlations. Peaks at 2.2 Å and higher r values are probably due to a contribution of several atom pairs. For the Gaussian fits, based again on the crystal structure, peaks at approximate positions of 1.1 (C–H), 1.4 (C–O), 1.5 (C–C), 1.7 (D–D), and 2.2 Å were included. Figure 3 illustrates the result for the molten PEO. The values obtained for the mean pair separations and coordination numbers are shown in Tables I and II. The mean pair separations for the room-temperature (semicrystalline) and 90 °C (liquid) samples are similar to values in the literature for crystalline PEO. The

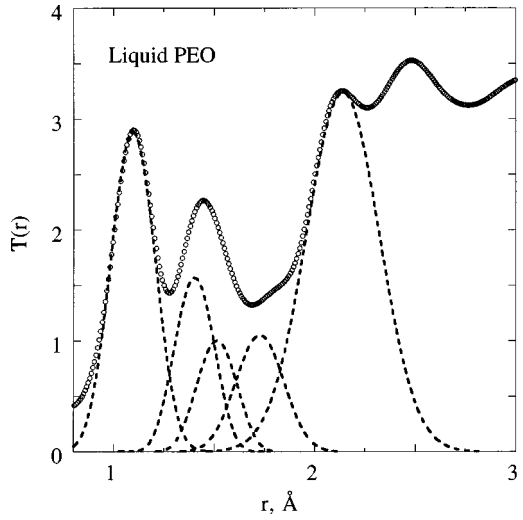

FIG. 3. Neutron-weighted average total correlation function for D-PEO at 90 °C: data (open circles) and fitted Gaussian functions (dashed line).

coordination numbers, however, show some differences, lower than the crystal for the C–D pairs but slightly higher for the C–O and C–C pairs.

The hydrogen-difference pair correlation function $g_H(r)$ was calculated from $S_H(Q)$ [Eq. (2)] by the Fourier transformation of Eq. (3), derived from the H- and D-PEO data at room temperature: in this quantity the C–O and C–C interactions are in principle eliminated and only correlations involving hydrogen should remain. The only clearly resolved peak corresponded to the C–H correlation and gave values for the C–H pair separation and coordination number consistent with those obtained from the $T(r)$ of D-PEO (Tables I and II).

IV. MOLECULAR DYNAMICS

The MD model is fully described in Ref. 11. Here we ran the simulation at a higher temperature in order to simulate the liquid sample measured at 90 °C. We first computationally repolymerized the sample at several different ''reaction rates'' (parameter τ in Ref. 11), then ran the simulation for 18 000 time steps (7.56 ps) and took data for 2000 more steps to obtain structural functions as described below. The simulations were run in the NVE (constant number, volume, and energy) ensemble with the average kinetic energy corresponding to 400 K as described previously.[11] By calculation of the mean-square displacement of atoms as a function of time we confirmed that the model was displaying liquidlike behavior on these (rather short) time scales. This is in contrast with our earlier simulations at 280 K in which the root-mean-square displacements saturated at values much smaller than the simulation box size on these time scales. Thus on these time and length scales the model is behaving like a liquid at 400 K, consistent with the experimental melting temperature. However, the structure obtained depends on the value used for τ in the simulation of the polymerization even at kinetic energies corresponding to 400 K. This indicates that the simulated liquid is not in equilibrium at all time and length scales. The final density for each simulation run was set to 1.06 g/cm^3 by adjustment of the sample box size.

TABLE I. Mean pair separations, R_{ij}(Å). The estimated uncertainties in the semicrystalline and liquid states are ±0.01 Å.

Atom pair	Crystal[a]	Semicrystalline	Liquid
C–D	1.09	1.10	1.09
C–O	1.43	1.43	1.40
C–C	1.54	1.50	1.51

[a]From Refs. 8 and 9.

TABLE II. Coordination numbers, $C_i(j)$. The estimated uncertainties in the semicrystalline and liquid states are ±0.2.

Atom pair	Crystal[a]	Semicrystalline	Liquid
C–D	2.0	1.7	1.4
C–O	1.0	1.1	1.0
C–C	1.0	1.1	1.2

[a]From Refs. 8 and 9.

Because this approach uses the united atom model for description of methyl and ethyl groups, it was necessary to develop a procedure for specifying the hydrogen positions in order to compare with the experimental results.[16] We chose to insert the hydrogen or deuterium entities during the simulation only when collecting data for the calculation of the relevant neutron-weighted average structure factors and pair correlation functions [Eqs. (1) and (3)]. The hydrogen/deuterium dynamics are not explicitly simulated. The reasons for this choice are the following: though the effects of the united atom model on structure and dynamics are not negligible, they are small, particularly on the time and length scales of interest in studying low-frequency conductivity and other properties of interest for battery applications. Long runs will be required for simulating these properties especially when adding explicitly the hydrogen motions and the quantum effects.

To calculate the neutron-weighted average $g(r)$, a set of hydrogen positions was determined at each time step for which data are collected, calculating the average structure functions by the following algorithm. First a ''tetrahedral position'' was assigned for each hydrogen; this is done uniquely for each carbon within a chain (but not at its ends) by determining the C–C–O plane to which the carbon belongs and then fixing the ''tetrahedral positions'' of the two associated hydrogen atoms in the plane perpendicular to this plane which bisects the C–C–O angle in it, with the bisector of the H–C–H bond along that bisector, with the H–C–H angle at the tetrahedral angle and with the C–H bond lengths at 1.68 Å [Fig. 4(a)]. For the end carbons, this procedure does not work; instead we calculate the C–O direction and fix ''tetrahedral positions'' for the three end deuterium atoms by placing a triad of C–H bonds at angles so that the C is at the center of a tetrahedron defined by the three H's and a (nonexistent) H along the C–O direction. The azimuthal orientation of the tetrahedron with respect to the C–O bond is set at random by choice of an azimuthal angle with equal probability for all values between 0 and 2π [Fig. 4(b)].

Even at zero temperature, the hydrogen positions deviate

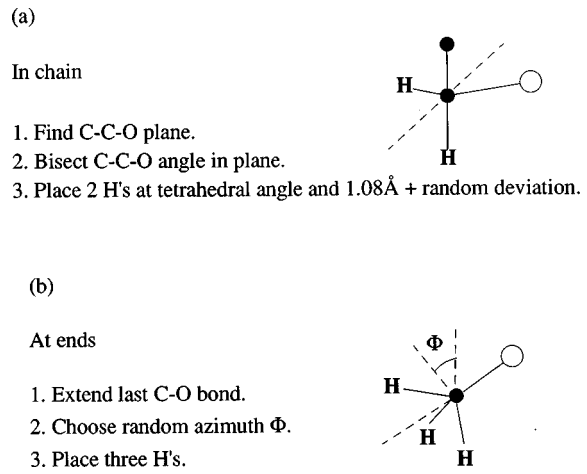

FIG. 4. Algorithm for determining hydrogen/deuterium positions in the MD simulations.

significantly from their ideal positions due to zero point motion. To take account of this effect we have added a random displacement to each ''tetrahedral'' hydrogen position described above. In the results reported here this random displacement is chosen from an isotropic Gaussian distribution of width 0.1 Å. A more realistic distribution based on the known harmonic frequencies of the CH_n groups could be instead used, and results using this procedure will be reported later. The present results indicate that this level of refinement is not required to account for experiments with the real-space resolution reported here.

In Fig. 5 the function $g(r)$ defined by Eqs. (1) and (3) is shown for two different values of the polymerization time τ. The functions are not identical, implying that the simulated liquid is not entirely at equilibrium, even though the real polymer is expected to be at equilibrium. Furthermore, the peaks are somewhat sharper than those observed in the experimental $g(r)$ (Fig. 2). However, if we take the finite experimental spatial resolution into account we can quite closely reproduce the experiments with these results. In Fig. 6 we compare the result of convoluting the $\tau=200$ fs result

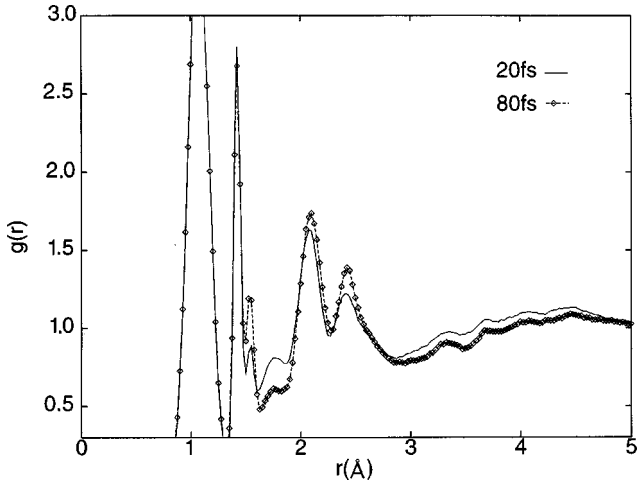

FIG. 5. Neutron-weighted average pair correlation function for D-PEO derived from the MD results for two values of the polymerization time τ.

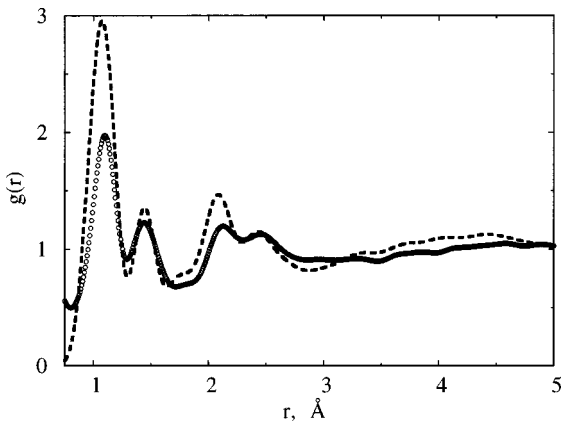

FIG. 6. Neutron weighted average pair correlation functions for D-PEO: data (open circles) and MD simulations (dashed line).

with a broadening function $M(r)$ [the Fourier transform of the window function $M(Q)$ with $Q_{\text{cut}}=30.0$ Å^{-1}] with the experimental results. Figure 7 shows the comparison of the back transform of the $\tau=200$ fs MD result with the experimental data for $S(Q)$.

Another approach is to compare the coordination numbers derived from the simulations with the experimental values for the molten PEO shown in Table II. An excellent agreement is obtained for C–C and C–O pairs while the calculated C–H coordination number (higher than two) is substantially larger than the experimental value. This is due to the unrealistically large number of unpolymerized end groups to which three hydrogen atoms were assigned.

V. DISCUSSION

There are relatively few results in the literature on wide-angle diffraction data from amorphous polymers. Carlsson *et al.*[17] have made neutron diffraction measurements on polypropylene oxide (PPO) which can be obtained in a purely amorphous form at room temperature. Their neutron-weighted average $S(Q)$ is qualitatively similar to that shown for PEO in Fig. 1, with pronounced peaks at 1.5 and 3.2 Å^{-1}.

The pair separations derived from the Gaussian fits to the PEO data (Fig. 3, Table I) are in good agreement with the

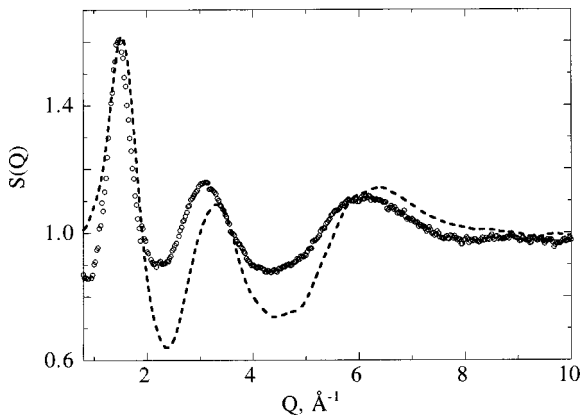

FIG. 7. Neutron weighted average structure factors for D-PEO: data (open circles) and MD simulations (dashed line).

values reported for crystalline PEO.[8,9] The coordination numbers derived from the peak areas (Table II) are also in reasonable agreement, except that the coordination number for the nearest neighbor C–D separation is significantly lower. There are a number of possible reasons for a reduced coordination number in a neutron diffraction measurement on a deuterated sample, including:

(a) significant Q resolution;
(b) Q-dependent noise in the measured intensity;
(c) an underestimated microscopic density ρ_0 which affects the coordination number via the second term in Eq. (4);
(d) a residual H content in the deuterated sample;
(e) a sample dependent background;
(f) broadening in real space due to the finite Q range.
(g) uncertainty in subtracting the self-scattering.

Of these possibilities, (a), (c), and (e) will affect all coordination numbers; (a) actually more for peaks at higher r, whereas the coordination numbers for the C–O and C–C peaks are, if anything, higher than the crystalline values. A 10% H:D ratio is estimated to reduce $C_C(D)$ by 14% and $C_C(O)+C_C(C)$ by about 2%, which would be sufficient to account for the result obtained for the semicrystalline sample. Item (b), Q-dependent noise, is the hardest to estimate since it will depend on how well the peak being fitted can be resolved from the $T(r)$ pattern. Numerical simulations performed on the data as well as investigations of the effect of varying Q_{cut} suggest that effects of about 15% would be quite possible and could be different for the semicrystalline and liquid data. Overall, the apparent reduction in $C_C(D)$ in going from the crystalline to the semicrystalline and liquid phases should not be regarded as significant.

The experimental $g(r)$ obtained from the PPO data of Carlsson *et al.* gave distances of 1.1, 1.5, and 1.8 Å for the C–D, (C–O+C–C), and H–H correlations, respectively.[17] The present data for PEO, like those for PPO,[17] indicate a short-range order very similar to that of the crystalline analogs. To obtain detailed information about the structure of amorphous PEO on an intermediate length scale, it is necessary to compare with computer simulation results such as the MD presented here.

Comparison of the simulation results with the data taken above the melting temperature shows good agreement (Figs. 6 and 7). This indicates broad consistency of the model with the real structure, even though the hydrogen/deuterium concentrations of the model and the real sample are quite different. Additional calculations in which only two deuterium atoms per carbon were added to the structure did not significantly affect the agreement between the experiment and the model. This suggests that this comparison is not very sensitive to the details of the hydrogen content. The discrepancy between MD and experiment in the Q range 3–5 $\mathrm{Å}^{-1}$ may result from the finite chain length in the simulation.

The most interesting structural problem is the determination of the structure of the amorphous regions when the sample is below the melting point. To bring the model and the experiment together to address this question we need to either produce a simulation which includes both amorphous and crystalline regions or find a way to subtract the contribution of the crystalline regions from the experimental data. A simulation large enough to include amorphous and crystalline regions of realistic size is not attainable in the near future. It may, however, be possible to develop methods for subtracting the crystalline contributions from the data in order to extract a signal attributable to the amorphous regions.

VI. CONCLUSIONS

The structure factors of both deuterated and protonated PEO were determined in the semicrystalline and liquid states to provide a precise measure of the short-range structural parameters. No differences were detected in the semicrystalline state between two polymers prepared with different molecular weights. We find good agreement in the liquid state with MD simulations based on the model of Ref. 11 and taking account of the presence of deuterium atoms in the structure. A discrepancy in the coordination number of the deuterium around the carbon centers is attributable in part to differences in deuterium concentration in the experiment and the simulation. It would be desirable to make a similar comparison between the model and the experiment for the amorphous parts of the semicrystalline sample below the melting point. Studies are also in progress on lithium-conducting salt-in-PEO solutions where MD simulations have been carried out[18] with potentials based on *ab initio* quantum-mechanical calculations.[19]

ACKNOWLEDGMENTS

This work was supported by the Divisions of Chemical Sciences and Materials Sciences, Office of Basic Energy Sciences, U. S. Department of Energy, under Contract No. W-31-109-ENG-38. Work at the University of Minnesota was supported by Department of Energy Basic Energy Sciences Grant No. DE-FG02-93ER14376 and the University of Minnesota Supercomputing Institute. The authors wish to thank L. A. Curtiss for discussions and sharing unpublished results. The diligent assistance of K. J. Volin during the neutron measurements is gratefully acknowledged.

[1] M. B. Armand, in *Polymer Electrolyte Review—I*, edited by J. R. MacCallum and C. A. Vincent (Elsevier Applied Science, New York, 1987), p. 1.
[2] M. A. Ratner and A. Nitzan, Faraday Discuss. Chem. Soc. **88**, 19 (1990).
[3] S. D. Druger, M. A. Ratner, and A. Nitzan, Mol. Cryst. Liq. Cryst. **190**, 171 (1990).
[4] M. Forsyth, V. A. Payne, M. A. Ratner, S. W. de Leeuw, and D. F. Shriver, Solid State Ionics **53–56**, 10011 (1992).
[5] A. Hooper, M. Gauthier, and A. Belanger, *Electrochemical Science and Technology of Polymers*, edited by R. G. Liford (Elsevier Applied Science, New York, 1990), p. 375.
[6] J. E. Weston and B. C. Steele, Solid State Ionics **2**, 347 (1981).
[7] C. Berthier, W. Gorecki, M. Minier, M. B. Armand, J. M. Chabgno, and P. Rigaud, Solid State Ionics **11**, 91 (1983).
[8] Y. Takahashi and H. Tadokoro, Macromolecules **6**, 672 (1973).
[9] T. P. Russell and H. Ito, Macromolecules **21**, 1703 (1988).
[10] J. Kugler, E. W. Fischer, M. Peuscher, and C. D. Eisenbach, Makromol. Chem. **184**, 2325 (1983).
[11] B. Lin, P. T. Boinske, and J. W. Halley, J. Chem. Phys. **105**, 1668 (1996).
[12] B. Lin and J. W. Halley, J. Phys. Chem. **99**, 16474 (1995).
[13] C. D. Eisenbach and M. Peuscher, Makromol. Chem., Rapid Commun. **1**, 105 (1980).

[14] C. D. Eisenbach, M. Peuscher, G. Wegner, and M. Weiss, Makromol. Chem. **184**, 2313 (1983).
[15] A. K. Soper and A. Luzar, J. Chem. Phys. **97**, 1320 (1993).
[16] J. W. Halley and B. Nielsen (unpublished).
[17] P. Carlsson, B. Mattson, J. Swenson, R. L. McGreevy, B. Gabrys, W. S. Howells, L. S. Boerjesson, and L. M. Torrell, Physica B **234–236**, 231 (1997); P. Carlsson, B. Mattson, J. Swenson, L. Boerjesson, L. M. Torrell, R. L. McGreevy, and W. S. Howells, Electrochim. Acta **43**, 1545 (1998).
[18] P. T. Boinske, L. A. Curtiss, J. W. Halley, B. Lin, and A. Sutjianto, J. Computer Aided Mater. Design **3**, 385 (1996).
[19] A. Sutjianto and L. A. Curtiss, Chem. Phys. Lett. **264**, 127 (1997).